

Nature of Magnetic Coupling between Mn Ions in As-Grown $\text{Ga}_{1-x}\text{Mn}_x\text{As}$ Studied by X-Ray Magnetic Circular Dichroism

Y. Takeda,^{1,*} M. Kobayashi,² T. Okane,¹ T. Ohkochi,¹ J. Okamoto,^{1,†} Y. Saitoh,¹ K. Kobayashi,^{1,§} H. Yamagami,^{1,7} A. Fujimori,² A. Tanaka,³ J. Okabayashi,^{4,‡} M. Oshima,⁴ S. Ohya,^{5,6} P.N. Hai,⁵ and M. Tanaka⁵

¹Japan Atomic Energy Agency, Synchrotron Radiation Research Center SPring-8, Sayo, Hyogo 679-5148, Japan

²Department of Physics, The University of Tokyo, Hongo, Tokyo 113-0033, Japan

³Graduate School of Advanced Sciences of Matter, Hiroshima University, Higashi-Hiroshima 739-8530, Japan

⁴Department of Applied Chemistry, The University of Tokyo, Hongo, Tokyo 113-8656, Japan

⁵Department of Electronic Engineering, The University of Tokyo, Hongo, Tokyo 113-8656, Japan

⁶PRESTO Japan Science and Technology Agency, Kawaguchi, Saitama 331-0012, Japan

⁷Department of Physics, Faculty of Science, Kyoto Sangyo University, Kyoto, 603-8555, Japan

(Received 29 November 2007; published 16 June 2008)

The magnetic properties of as-grown $\text{Ga}_{1-x}\text{Mn}_x\text{As}$ have been investigated by the systematic measurements of temperature and magnetic field dependent soft x-ray magnetic circular dichroism (XMCD). The *intrinsic* XMCD intensity at high temperatures obeys the Curie-Weiss law, but a residual spin magnetic moment appears already around 100 K, significantly above the Curie temperature (T_C), suggesting that short-range ferromagnetic correlations are developed above T_C . The present results also suggest that the antiferromagnetic interaction between the substitutional and interstitial Mn (Mn_{int}) ions exists and that the amount of the Mn_{int} affects T_C .

DOI: 10.1103/PhysRevLett.100.247202

PACS numbers: 75.50.Pp, 75.25.+z, 78.70.Dm, 79.60.Dp

$\text{Ga}_{1-x}\text{Mn}_x\text{As}$ is a prototypical and most well-characterized diluted magnetic semiconductor (DMS) [1]. Because $\text{Ga}_{1-x}\text{Mn}_x\text{As}$ is grown under thermal nonequilibrium conditions, however, it is difficult to avoid the formation of various kinds of defects and/or disorders. In fact, Rutherford backscattering (RBS) channeling experiments for as-grown $\text{Ga}_{0.92}\text{Mn}_{0.08}\text{As}$ samples have shown that as many as $\sim 17\%$ of the total Mn ions may occupy the interstitial sites [2]. It is therefore supposed that the antiferromagnetic (AF) interaction between the substitutional Mn (Mn_{sub}) ions and interstitial Mn (Mn_{int}) ions may suppress the magnetic moment [3,4]. In addition, the random substitution of Mn ions may create inhomogeneous Mn density distribution, which may lead to the development of ferromagnetic domains above Curie temperature (T_C) [5]. The characterization of nonferromagnetic Mn ions is therefore a clue to identify how they are related with the ferromagnetic ordering and eventually to improve the ferromagnetic properties of $\text{Ga}_{1-x}\text{Mn}_x\text{As}$ samples. However, it has been difficult to extract the above information through conventional magnetization measurement due to the large diamagnetic response of the substrate and the unavoidable mixture of magnetic impurities.

X-ray magnetic circular dichroism (XMCD), which is an element specific magnetic probe, is a powerful technique to address the above issues. So far, several results of XMCD measurements on $\text{Ga}_{1-x}\text{Mn}_x\text{As}$ have been reported [6–8]. From magnetic field (H) dependent XMCD studies, the enhancement of XMCD intensity by post-annealing implies AF interaction between the Mn_{sub} and Mn_{int} ions has been proposed [8]. In the present study, in order to characterize the magnetic behaviors of the Mn_{sub} and Mn_{int} , we

have extended the approach and performed systematic temperature (T) and H dependent XMCD studies in the Mn $L_{2,3}$ absorption edge region of $\text{Ga}_{1-x}\text{Mn}_x\text{As}$. The systematic dependences of XMCD signals help us to obtain important information about details of magnetic properties, namely, characteristic behaviors of the ferromagnetic and paramagnetic components of a specific magnetic element and even magnetic interaction between them, on a microscopic level [9,10]. We have also found that short-range ferromagnetic correlations develop significantly above T_C and that AF interaction between the Mn_{sub} and Mn_{int} is important to understand the magnetic properties of $\text{Ga}_{1-x}\text{Mn}_x\text{As}$.

We prepared two as-grown samples with different Mn concentrations, $x = 0.042$ and 0.078 , whose T_C was ~ 60 and 40 K, respectively, as determined by an Arrott plot of the anomalous Hall effect. To avoid surface oxidation, the sample had been covered immediately after the growth of $\text{Ga}_{1-x}\text{Mn}_x\text{As}$ films by cap layers without exposure to air [As cap/GaAs cap(1 nm)/ $\text{Ga}_{1-x}\text{Mn}_x\text{As}$ (20 nm)/GaAs(001)]. The x-ray absorption spectroscopy (XAS) and XMCD measurements were performed at the helical undulator beam line BL23SU of SPring-8 [11,12]. The XAS spectra were obtained by the total-electron yield mode. The measurements were done without a surface treatment and H was applied to the sample perpendicular to the film surface.

Figures 1(a) and 1(b) show the XAS spectra (μ^+ and μ^-) in the photon energy region of the Mn L_3 absorption edge and the corresponding XMCD spectra, defined as $\mu^+ - \mu^-$, at $T = 20$ K and $H = 0.5$ T for $x = 0.042$ and 0.078 . Here, μ^+ (μ^-) refers to the absorption coefficient

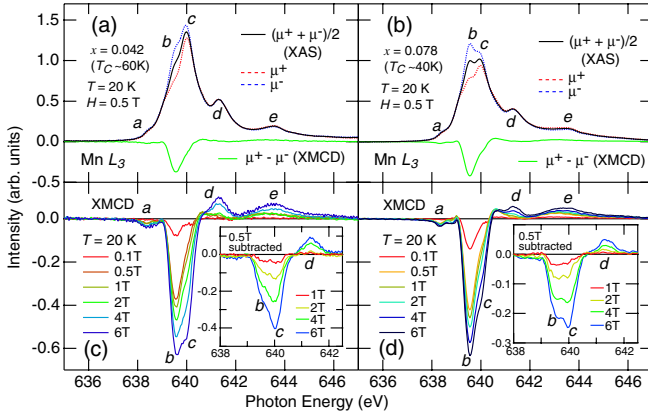


FIG. 1 (color online). Mn L_3 -edge XAS [μ^+ , μ^- and $(\mu^+ + \mu^-)/2$] and XMCD ($\mu^+ - \mu^-$) spectra of $\text{Ga}_{1-x}\text{Mn}_x\text{As}$ taken at $T = 20$ K and $H = 0.5$ T for $x = 0.042$ (a) and $x = 0.078$ (b). Panels (c) and (d) show the H dependence of the XMCD spectra for $x = 0.042$ and $x = 0.078$, respectively. Inset shows the difference XMCD spectra obtained by subtracting the XMCD spectrum at $H = 0.5$ T.

cient for the photon helicity parallel (antiparallel) to the Mn $3d$ majority spin direction. The XAS spectra for both Mn concentrations have five structures labeled as a , b , c , d , and e . The average XAS spectra [defined by $(\mu^+ + \mu^-)/2$] have been normalized to 1 at structure b . The intensity ratio c/b is very different between $x = 0.042$ and 0.078 , indicating that the spectra consist of two overlapping components. Figures 1(c) and 1(d) show the H dependence of the XMCD spectra. As H increases, XMCD structures corresponding to structures c , d , and e are enhanced, particularly, strongly for the $x = 0.042$ sample. One can see this behavior more clearly in the difference XMCD spectra obtained by subtracting the XMCD spectrum at 0.5 T from the spectra at $H = 1, 2, 4$, and 6 T as shown in the inset of Figs. 1(c) and 1(d). Recent XAS and XMCD studies have revealed that these structures (c, d, e) are ascribed to contamination of out-diffused Mn ions on the surface [7,13,14]. The difference in the XAS intensity ratio c/b is therefore naturally ascribed to the difference in the amount of Mn ions diffused into the cap layer or the surface region during the growth of GaAs on $\text{Ga}_{1-x}\text{Mn}_x\text{As}$. In the following, therefore, we shall neglect those extrinsic signals and focus only on intrinsic signals, particularly structure b , to investigate the intrinsic magnetic behavior.

In order to extract the *intrinsic* XAS spectrum, we assumed that structure b could be ascribed to the intrinsic Mn ions as mentioned above. Therefore, we first obtained the *extrinsic* XAS spectrum as $(\text{XAS } x = 0.042) - p(\text{XAS } x = 0.078)$, where p was chosen so that structure b vanished. The *intrinsic* XAS spectrum was then obtained as $(\text{raw XAS}) - q(\text{extrinsic XAS})$, where q was determined so that the line shape of the *intrinsic* XAS spectrum agreed with that obtained from the fluorescence yield measurements [13,14]. Next, in order to extract the *intrinsic*

XMCD spectra, we first obtained the *extrinsic* XMCD spectrum as $(\text{XMCD at } 6\text{ T}) - \alpha(\text{XMCD at } 0.5\text{ T})$, where α was chosen so that an XMCD structure corresponding to structure b vanished by utilizing the fact that the ferromagnetic signals and hence the intrinsic signals should be dominant in the XMCD spectrum at low H . The *intrinsic* XMCD spectrum was then obtained as $(\text{XMCD at each } H) - \beta(\text{extrinsic XMCD spectrum})$, where β was chosen so that structure c vanished. Figures 2(a) and 2(b) show the results of the decomposition of the XAS and XMCD spectra into the intrinsic and extrinsic components for $x = 0.042$ and 0.078 , respectively. While the XMCD intensity is enhanced as H increases and T decreases, the line shapes of the *intrinsic* XMCD spectra are unchanged with H and T . The line shapes of the *intrinsic* XAS and XMCD spectra for both Mn concentrations thus agree with each other as shown in Fig. 2(c), indicating that the decomposition procedure was valid.

Using the *intrinsic* XAS and XMCD spectra, we have applied the XMCD sum rules [15,16], assuming the Mn $3d$ electron number $N_d = 5.1$ [8], and estimated the spin magnetic moment (M_S) at $T = 20$ K and $H = 0.5$ T to be $M_S = 2.5 \pm 0.2$ and 1.7 ± 0.2 (μ_B per Mn) for $x = 0.042$ and 0.078 , respectively. These M_S values are much larger than those obtained in the early studies on oxidized surfaces [6] and comparable to the recent ones on etched surfaces [8], indicating that the cap layer protected the ferromagnetic properties of $\text{Ga}_{1-x}\text{Mn}_x\text{As}$. The ratio M_L/M_S is estimated to be 0.07 for both concentrations, where M_L is the value of the orbital magnetic moment, showing that the intrinsic Mn ion has a finite, although small, M_L , probably because of certain deviation from the pure Mn^{2+} (d^5) state.

The T dependence of M_S from the XMCD signal for $H = 6$ T is plotted in Fig. 3(a). As T decreases, the XMCD signal increases monotonically except for the discontinuity at around T_C (~ 60 K for $x = 0.042$, ~ 40 K for $x = 0.078$). This discontinuity probably reflects the ferromag-

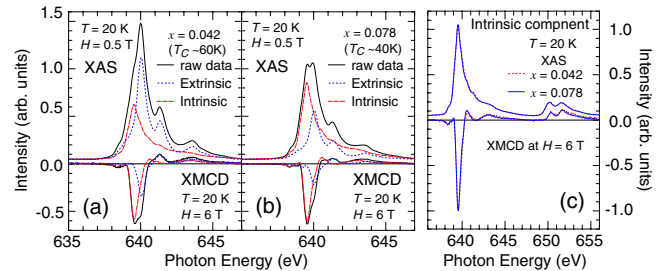


FIG. 2 (color online). Decomposition of the XAS and XMCD spectra of $\text{Ga}_{1-x}\text{Mn}_x\text{As}$ into the intrinsic and extrinsic components for $x = 0.042$ (a) and for $x = 0.078$ (b) in the Mn L_3 edge region. Panel (c) shows comparison of the line shapes of the *intrinsic* XAS and XMCD spectra between $x = 0.042$ and 0.078 , normalized to the peak heights.

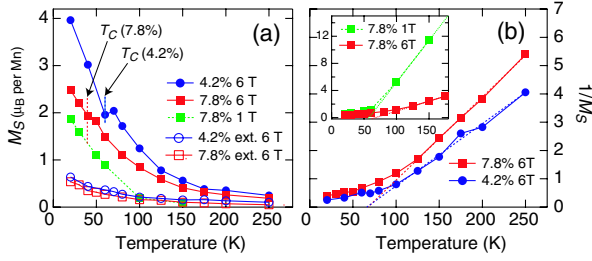


FIG. 3 (color online). T dependence of the spin magnetic moment M_S . (a) T dependence of M_S for $H = 6$ T. For $x = 0.078$, results for $H = 1$ T are also plotted. Open symbols show that of the extrinsic component at $H = 6$ T. (b) T dependence of the inverse of M_S . Inset shows comparison between 1 and 6 T for $x = 0.078$.

netic ordering which aligns the magnetization parallel to the sample surface, the easy axis of magnetization in the films [17]. It should be noted that M_S increases monotonically even well below T_C as T decreases, indicating that full spin polarization is not achieved even well below T_C . For $x = 0.078$, the T dependence for $H = 1$ T shows essentially the same behavior as that for 6 T. Figure 3(b) shows the inverse of M_S plotted in Fig. 3(a). The high-temperature part is well described by the Curie-Weiss (CW) law, independent of H as shown in the inset of Fig. 3(b).

Figure 4 shows the H dependence of M_S at several temperatures for $x = 0.042$ [panel (a)] and 0.078 [panel (b)]. M_S of the intrinsic component is increased rapidly from $H = 0.1$ to 0.5 T at $T = 20$ K, due to the reorientation of the ferromagnetic moment from the in-plane to out-of-plane directions [17]. Above 0.5 T, M_S is increased almost linearly as a function of H . We have plotted the T dependence of $M_S|_{H \rightarrow 0}$ T obtained from the linear extrapolation of M_S at high fields to $H = 0$ T and

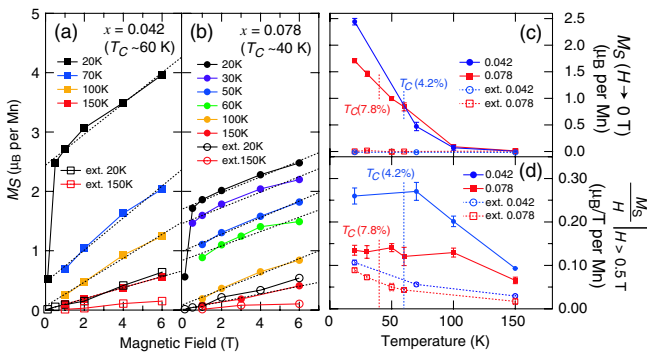


FIG. 4 (color online). H dependence of M_S for $x = 0.042$ (a) and for $x = 0.078$ (b) at several temperatures. Dashed lines show fitted straight lines above 0.5 T. (c) T dependence of the residual magnetization $M_S|_{H \rightarrow 0}$ T (M_S for $H \rightarrow 0$ T). Open symbols show that of the extrinsic component. (d) T dependence of the slope of the M_S - H curve above 0.5 T, i.e., the high-field magnetic susceptibility ($\partial M_S / \partial H|_{H > 0.5}$ T). Open symbols show that of the extrinsic component.

$\partial M_S / \partial H|_{H > 0.5}$ T (μ_B / T per Mn) (the susceptibility of the paramagnetic component) in Figs. 4(c) and 4(d), respectively. For the extrinsic component, $M_S|_{H \rightarrow 0}$ T is vanishingly small at all temperatures and $\partial M_S / \partial H|_{H > 0.5}$ T is increased as T decreases following the CW law, indicating that the extrinsic component is paramagnetic and decoupled from the ferromagnetism of the intrinsic component. As for the ferromagnetic component, $M_S|_{H \rightarrow 0}$ T is steeply increased below ~ 100 K, i.e., from somewhat above T_C . The T dependence of $M_S|_{H \rightarrow 0}$ T [Fig. 4(c)] is correlated with the deviation from the CW law below ~ 100 K [Fig. 3(b)]. Well below T_C , $M_S|_{H \rightarrow 0}$ T still continues to increase with decreasing T , indicating the inhomogeneous nature of the ferromagnetism. As for $\partial M_S / \partial H|_{H > 0.5}$ T, unlike the extrinsic component, it saturates around T_C and is not increased as T further decreases. The appearance and increase of $M_S|_{H \rightarrow 0}$ T between T_C and ~ 100 K [Fig. 4(c)] strongly suggest that short-range ferromagnetic correlations start to develop and ferromagnetic domains form before the long-range order is established at *macroscopic* T_C . Each ferromagnetic domain may have different ferromagnetic behavior due to the spatial distribution of T_C in the as-grown samples. Those results may correspond to the theoretical prediction that ferromagnetic domains develop above T_C when there is magnetic inhomogeneity [5].

The suppression of the CW-like increase of $\partial M_S / \partial H|_{H > 0.5}$ T below T_C in both samples indicates AF interaction between the ferromagnetic Mn, i.e., Mn_{sub} and nonferromagnetic (or paramagnetic) Mn such as Mn_{int} . The recent H dependent XMCD study of $Ga_{1-x}Mn_xAs$ shows that $\partial M_S / \partial H|_{H > 0.5}$ T becomes small and $M_S|_{H \rightarrow 0}$ T becomes large after post-annealing, suggesting that the changes are caused by a reduction of Mn_{int} [8]. In the present study, $\partial M_S / \partial H|_{H > 0.5}$ T and $M_S|_{H \rightarrow 0}$ T are smaller for $x = 0.078$ than for $x = 0.042$ [Figs. 4(c) and 4(d)], suggesting that AF interaction becomes stronger for $x = 0.078$ than that for $x = 0.042$. This is reasonable because the number of Mn_{int} is expected to be larger for larger Mn concentration. Assuming that M_S per the Mn_{sub} is 5 (μ_B per Mn) and M_S of the Mn_{int} is antiparallel to that of Mn_{sub} , the ratio of Mn_{int} ions in the intrinsic component (R_{int}) is estimated as 0.26 for $x = 0.042$ and 0.33 for $x = 0.078$ from $M_S|_{H \rightarrow 0}$ T at $T = 20$ K. This is consistent with the result of the RBS experiment [2], which R_{int} is estimated as 0.17 for an as-grown sample with $T_C = 67$ K, indicating that T_C is strongly correlated with the amount of Mn_{int} . We have fitted the susceptibility $\partial M_S / \partial H|_{H = 6}$ T (μ_B / T per Mn) of the intrinsic component above 100 K [Fig. 3(b)] to the CW law with an offset, $\partial M_S / \partial H|_{H = 6}$ T = $N_x C / (T - \Theta) + \partial M_S / \partial H|_0$, where $C = (g \mu_B)^2 S(S + 1) / 3k_B$ is the Curie constant, Θ is the Weiss temperature, $\partial M_S / \partial H|_0$ is the constant offset, N_x is the number of magnetic Mn ions in the sample with Mn concentration x , and g is the g factor. Θ is estimated to be 68 ± 5 K for

$x = 0.042$ and 69 ± 3 K for $x = 0.078$. $\partial M_S / \partial H|_0$ is estimated to be of the order of $\sim 10^{-3}$ for both samples. Assuming $g = 2$, $S = 5/2$ and $\Theta = 68$ K, one obtains $N_{0.042} = 0.97$ and $N_{0.078} = 0.67$. This result strongly suggests that most of the intrinsic Mn ions in the $x = 0.042$ sample participate in the paramagnetism above ~ 100 K, and the paramagnetism in the $x = 0.078$ sample is suppressed even at high temperatures, again implying that the AF interaction is stronger and more influential in the $x = 0.078$ sample.

In conclusion, we have investigated the T , H and Mn concentration dependences of the ferromagnetism in as-grown $\text{Ga}_{1-x}\text{Mn}_x\text{As}$ samples by XMCD measurements to extract the intrinsic magnetic component. The XMCD intensity deviates from the CW law below ~ 100 K, indicating that the ferromagnetic moment starts to form at ~ 100 K and that the short-range ferromagnetic correlations develop significantly above T_C . The high-field magnetic susceptibility becomes T -independent below T_C , indicating that the AF interaction between the Mn_{sub} and Mn_{int} ions, which becomes strong as the Mn concentration x increases, plays an important role to determine the magnetic behavior of $\text{Ga}_{1-x}\text{Mn}_x\text{As}$. In addition, the amount of the Mn_{int} ions should be strongly related with T_C . The present experimental findings should give valuable insight into the inhomogeneous magnetic properties of many DMS's. In future studies, it is very important to perform a detail T and H dependent XMCD study for a post-annealed samples.

This work was performed under the Proposal No. 2006A3817 at SPring-8 BL23SU and supported partly by Grants-in-Aids for Scientific Research in Priority Area "Semiconductor Spintronics" (No. 14076209), "Creation and Control of Spin Current" (No. 190481012) and by PRESTO/SORST of JST, "Special Coordination Programs for Promoting Science and Technology," and "Next-Generation IT Program" from the Ministry of Education, Culture, Sports, Science and Technology.

*ytakeda@spring8.or.jp

†National Synchrotron Radiation Research Center, 101 Hsin-Ann Road, Hsinshuu Science Park, Hsinchu 30077, Taiwan, R. O. C.

‡Department of Physics, Tokyo Institute of Technology, Ookayama, Meguro-ku, Tokyo 152-8551, Japan

§National Institute for Materials Science, SPring-8, Sayo, Hyogo 679-5198, Japan

- [1] H. Ohno, *Science* **281**, 951 (1998).
- [2] K. M. Yu, W. Walukiewicz, T. Wojtowicz, I. Kuryliszyn, X. Liu, Y. Sasaki, and J. K. Furdyna, *Phys. Rev. B* **65** 201303(R) (2002).
- [3] J. Blinowski and P. Kacman, *Phys. Rev. B* **67**, 121204(R) (2003).
- [4] J. Mašek and F. Maca, *Phys. Rev. B* **69**, 165212 (2004).
- [5] M. Mayr, G. Alvarez, and E. Dagotto, *Phys. Rev. B* **65** 241202(R) (2002).
- [6] H. Ohldag, V. Solinus, F. U. Hillebrecht, J. B. Goedkoop, M. Finazzi, F. Matsukura, and H. Ohno, *Appl. Phys. Lett.* **76**, 2928 (2000).
- [7] K. W. Edmonds, N. R. S. Farley, R. P. Campion, C. T. Foxon, B. L. Gallagher, T. K. Johal, G. van der Laan, M. MacKenzie, J. N. Chapman, and E. Arenholz, *Appl. Phys. Lett.* **84**, 4065 (2004).
- [8] K. W. Edmonds, N. R. S. Farley, T. K. Johal, G. van der Laan, R. P. Campion, B. L. Gallagher, and C. T. Foxon, *Phys. Rev. B* **71**, 064418 (2005).
- [9] M. Kobayashi, Y. Ishida, J. I. Hwang, T. Mizokawa, A. Fujimori, K. Mamiya, J. Okamoto, Y. Takeda, T. Okane, Y. Saitoh, Y. Muramatsu, A. Tanaka, H. Saeki, H. Tabata, and T. Kawai, *Phys. Rev. B* **72**, 201201(R) (2005).
- [10] Y. Ishida, J. I. Hwang, M. Kobayashi, Y. Takeda, K. Mamiya, J. Okamoto, S.-I. Fujimori, T. Okane, K. Terai, Y. Saitoh, Y. Muramatsu, A. Fujimori, A. Tanaka, H. Saeki, T. Kawai, and H. Tabata, *Appl. Phys. Lett.* **90**, 022510 (2007).
- [11] A. Yokoya, T. Sekiguchi, Y. Saitoh, T. Okane, T. Nakatani, T. Shimada, H. Kobayashi, M. Takao, Y. Teraoka, Y. Hayashi, S. Sasaki, Y. Miyahara, T. Harami, and T. A. Sasaki, *J. Synchrotron Radiat.* **5**, 10 (1998).
- [12] Y. Saitoh, T. Nakatani, T. Matsushita, A. Agui, A. Yoshigoe, Y. Teraoka, and A. Yokoya, *Nucl. Instrum. Methods Phys. Res., Sect. A* **474**, 253 (2001).
- [13] Y. Ishiwata, T. Takeuchi, R. Eguchi, M. Watanabe, Y. Harada, K. Kanai, A. Chainani, M. Taguchi, S. Shin, M. C. Debnath, I. Souma, Y. Oka, T. Hayashi, Y. Hashimoto, S. Katsumoto, and Y. Iye, *Phys. Rev. B* **71**, 121202(R) (2005).
- [14] D. Wu, D. J. Keavney, Ruqian Wu, E. Johnston-Halperin, D. D. Awschalom, and Jing Shi, *Phys. Rev. B* **71**, 153310 (2005).
- [15] B. T. Thole, P. Carra, F. Sette, and G. van der Laan, *Phys. Rev. Lett.* **68**, 1943 (1992).
- [16] P. Carra, B. T. Thole, M. Altarelli, and X. Wang, *Phys. Rev. Lett.* **70**, 694 (1993).
- [17] H. Ohno, A. Shen, F. Matsukura, A. Oiwa, A. Endo, S. Katsumoto, and Y. Iye, *Appl. Phys. Lett.* **69**, 363 (1996).